

DETECTION OF SPONTANEOUS ACTION POTENTIALS IN EXTRACELLULAR RECORDINGS OF VISUAL CORTEX NEURONS USING EEG PREDICTORS FOR A MACHINE LEARNING-BASED APPROACH

O.S. Idzhilova*, I.V. Smirnov, A.Yu. Malyshev

Institute of Higher Nervous Activity and Neurophysiology of RAS, Moscow, Russia

* Corresponding author: olgaidzh@gmail.com

Abstract. Spontaneous activity is known to be a characteristic feature of the vast majority of the neocortical principal cells including neurons of the primary sensory areas. The question of how spontaneous activity interacts with perception and encoding of sensory information remains open. In the present study, pyramidal neurons of the mouse primary visual cortex were recorded extracellularly under urethane anesthesia and simultaneous single-channel EEG recording was performed. To evaluate orientation and direction selectivity of the recorded neurons, mice were presented with visual stimuli consisting of moving sinusoidal gratings of different orientations displayed on a monitor. We noted quite regular bursts of generalized brain activity that were manifested in the recorded neuron as bundles of action potentials accompanied with a distinctive EEG pattern. Clearly, whenever such spontaneous activity shows up during visual stimulation, it is considered as noise, which significantly compromises the characteristics of the neuron's measured visual response. To eliminate this effect, we developed a machine learning-based algorithm that enables to identify EEG predictors of generalized spontaneous activity and then to exclude spontaneous (i.e. not evoked by visual stimulation) action potentials from the recording. Our algorithm was shown to reliably detect action potentials that have been caused by generalized brain activity. Removal of action potentials of this origin from extracellular recordings obtained during visual stimulation allows for a more adequate estimation of parameters of neuronal receptive fields, in particular their orientation selectivity.

Keywords: primary visual cortex, spontaneous activity, orientation selectivity, EEG, wavelet transform, support vector machine, machine learning.

List of Abbreviations

AP – Action potential
EEG – Electroencephalogram
V1 – Primary visual cortex
SVM – Support Vector Machine
OSI – Orientation Selectivity Index
DSI – Direction Selectivity Index

Introduction

Brain never sleeps-even when the rest of the body seemingly does, central nervous system is constantly processing both internal information (somatic and psychical, including memory consolidation) and relevant external signals (McVea *et al.*, 2016). It is notable that neural network activity is able to propagate between brain regions, both horizontally (across cortex areas (Luczak *et al.*, 2007) and vertically (e.g., stem-cortex influences (Krone *et al.*, 2021). Widespread activity propagation involves areas that are presumably passive during sleep, for example primary visual

cortex, which, as its name suggests, performs low-level feature analysis of incoming visual stimuli. Cortical spontaneous activity is viewed as an off-line mode of information processing (Luczak *et al.*, 2007). In visual stimulation experiments, when it is desirable to isolate neuron's responses to presented stimuli, spontaneous activity acts as background noise. To deal with it, usually average spontaneous firing rate is computed within a short preceding window. Then it is subtracted from the firing rate of the response (Mazurek *et al.*, 2014). However, such approach is of little use in many instances, when spontaneous activity of V1 cell is highly irregular, coming and passing as bursts of action potentials, similar to sensory-evoked activity. Therefore, there is a need to investigate whether advent of individual bursts can be predicted from general brain state. Specifically, in this study, we tried to retrieve information about spontaneous burst inception in a primary visual cortex neuron

from EEG recorded simultaneously from a different cortex region. We managed to achieve > 70% accuracy of prediction from wavelet transformed EEG features fed into SVM classifier. Then, on visual stimulation recordings, classification of action potentials into “spontaneous” and “of other origin” was performed and the former were excluded, whereupon orientation selectivity index of the cell improved. Thus, we suggest that our algorithm can be utilized to clean extracellular recordings made during stimulation from spontaneous bursts.

Methods

Animals. All experimental procedures involving the animals conformed to the National Institute’s of Health Guide for the Care and Use of Laboratory Animals and were approved by the Institute’s of Higher Nervous Activity and Neurophysiology of RAS Ethical Committee. Adult C57Black/6J mice (1.5–4 month old, 21–30 g) were anesthetized with urethane (0.7–1 g/kg body weight) intraperitoneally. Under local lidocaine anesthesia, a metal fixator was attached to the exposed skull bone above the primary visual cortex (4.5 mm posterior, 2.5 mm lateral to the Bregma) and the skull was penetrated with a thin syringe needle.

EEG was recorded from a single stainless wire macroelectrode that was screwed into the skull bone above the left parietal area, and the reference silver wire electrode was placed above the cerebellum.

In vivo electrophysiological experiments. Visual stimuli consisted of moving sinusoidal luminance gratings (spatial frequency of 0.04 cycles/degree, speed of 2 Hz) of 12 orientations, presented on a 19-diagonal LCD monitor. Pseudorandom sequence was repeated in 30 trials and included 12 presentations that lasted for two seconds each, with 3 seconds between the onsets of two subsequent stimuli. For each cell, 10–40 minute recording of pure spontaneous activity, without any sensory stimulation, was performed as well.

Extracellular recordings were performed on eight cells, on four mice in total. Glass recording pipettes were filled with HBSS buffer. Elec-

trodes were placed in granular and infragranular layers (0.4–0.7 mm deep). Electrode of 4–12 M Ω was slowly descended through tissue until its resistance increased 1.5–2-fold upon cell contact set up. Responses were recorded by Multiclamp 700B amplifier (Molecular Devices, USA) with PClamp 10 software (Molecular Devices, USA), and the output was filtered at 300–10,000 Hz and digitized at 20 kHz (Digidata 1550 Series, Molecular Devices, USA). Single-electrode EEG was recorded simultaneously using the same software.

Wavelet transform of EEG. First, a training set was created as follows (al-Qerem et al., 2020). 1.2 second long epochs were extracted from EEG and divided into two classes, “spontaneous” and “silent”. Each spontaneous epoch was centered around one of the action potentials, and the only condition for the silent epochs was that there appeared no action potentials during them. Then, for each epoch, a set of features was created, from a set of discrete wavelet transform coefficients for that EEG snippet, in seven frequency bands (78.1–156.2 Hz, 39.1–78.1 Hz, 19.5–39.1 Hz, 9.8–19.5 Hz, 4.9–9.8 Hz, 2.4–4.9 Hz, 1.2–2.4 Hz and < 1.2 Hz). Wavelet function we used was a fourth order symlet (PyWavelets package for Python (Lee et al., 2019)). The transform was applied to a six second long EEG episode centered around each 1.2 s epoch. The features extracted were max and min values and their time coordinates, mean and standard deviation of wavelet coefficients (for the first four frequency bands), and max, min and mean for the last three bands, resulting in a feature vector of length 39. Dataset was then balanced by random exclusion of samples until the two class sizes became equal. Number of training samples varied in the range 100–1000 for all the cells.

Support Vector Machine classifier. Then, the training set data were centered and scaled (mean subtracted and the result divided by standard deviation of the set), split into training and test sets (70% and 30%) and the former fed into SVM classifier (Support Vector Classifier,

Scikit-learn package (Pedregosa et al., 2011)) with a radial basis function kernel, to perform a supervised training. The model was 5-fold cross-validated, with two parameters being optimized: regularization parameter ($C = 5$) and gamma (0.01–0.05). Then, classification of EEG recorded during stimulation was performed, within a sliding 1.2 second window, in 0.3 s steps. In this manner, for each datapoint we got four binary predictions (0, for the first class or 1, for the second) and calculated the average value (between 0 and 1), which was a conservative estimate of this point belonging to the second class of EEG episodes. Then, finally, we classified action potentials in the stimulation recording into two groups: “spontaneous” and “of other origin”, based on this estimate, with a threshold of 0.5. Those action potentials classified as spontaneous were excluded from further calculations of corrected index values.

Selectivity indices. To quantify the primary visual cortex neurons’ sensitivity to the stimulus properties (orientation and direction of movement), for each cell, standard normalized selectivity indices were calculated, defined as $OSI = (R_{pref} + R_{null} - (R_{(orth+)} + R_{(orth-)})) / (R_{pref} + R_{null})$ (orientation selectivity index) and $DSI = (R_{pref} - R_{null}) / (R_{pref} + R_{null})$ (direction selectivity index) (Mazurek et al., 2014), where R_{pref} is the response at the preferred orientation, as the best of all responses, $R_{(orth+)}$ and $R_{(orth-)}$ are the responses at the orientations that are orthogonal to the preferred one. Response is calculated as evoked firing rate – the number of APs evoked by the stimulus divided by its duration. Indices’ change as a result of the cleansing procedure is measured as $\Delta DSI = [DSI]_{after} - [DSI]_{before}$, $\Delta OSI = [OSI]_{after} - [OSI]_{before}$, where “before” and “after” correspond to index values before and after the algorithm has been applied.

Results

Spontaneous bursts of APs in V1 are accompanied with a characteristic EEG pattern in the parietal cortex area. While recording from V1 neurons, we monitored a single-channel EEG

recorded from the parietal cortex. In absence of external visual stimulation, in most of the recorded neurons we observed spontaneous activity in the form of regular bursts of APs. Interestingly enough, these bursts tended to be accompanied with a characteristic EEG pattern (Fig. 1) that incorporates both high- and low-frequency components. Its averaged general shape is shown in Fig. 2.

EEG snippets can be reliably classified based on ongoing spontaneous neuronal activity. Assuming that these two phenomena are related and might have a common origin, we estimated their interconnection. For each neuron, we trained a Support vector machine classifier to discriminate between “spontaneous” and “silent” EEG snippets (see Methods), labeled so depending on whether each episode was accompanied with spontaneous activity. Discrete wavelet transform was applied to extract a small number of meaningful features from a set of frequency bands for each EEG episode, thus reducing the dimensionality. Symlet was chosen for its shape being similar to the one of the EEG pattern (Fig. 2), and for its orthogonality property. SVM algorithms search for a hyperplane to separate the vectors of two classes, so that the margin is the largest possible. As there was a significant overlap between our two classes, maintaining the least false positive rate was paramount. A conservative separating border satisfied this requirement well. Radial basis kernel was preferred, as the data were not linearly separable.

Average classification results are presented in Table 1. Our algorithm enabled to achieve good enough classification accuracies of more than 70%. According to PCA, most of the features were evenly important for classification, so we chose to omit any further dimensionality reduction.

Classification accuracy significantly dropped to near chance values, when we ran the trained model on the data recorded from a different animal. This suggests that the observed EEG patterns are unique across different subjects. On the other hand, model achieved average classification accuracy of $62 \pm 3\%$ when

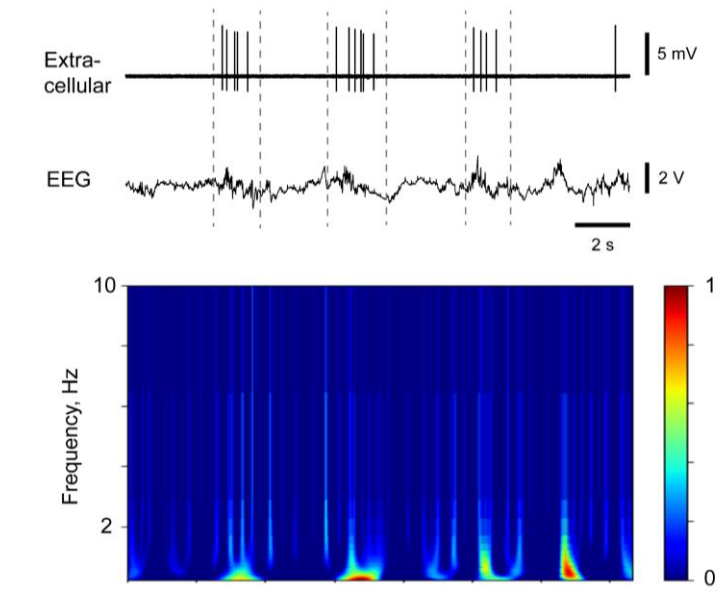


Fig. 1. Spontaneous APs come in bursts often accompanied with a distinctive EEG “comb” pattern. An example of extracellular recording of a single mouse V1 neuron (top), accompanied with EEG showing characteristic “combs” (middle) and its Gauss wavelet transform (bottom). Dashed lines mark approximate bursts’ boundaries. Colorscale represents normalized absolute wavelet transform coefficient value

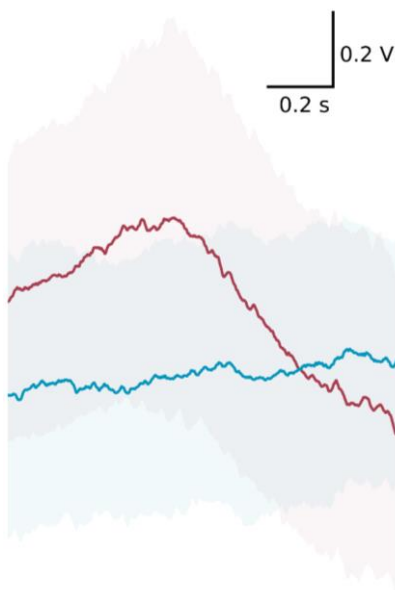


Fig. 2. Averaged EEG shapes. Averaged 1.2 second long EEG epochs corresponding to either spontaneous bursts (“burst-triggered average”, red), or silent periods (blue), for one of the analyzed cells. Shading covers one standard deviation. n = 1000 epochs. Here, a burst was determined as a sequence of action potentials in which the distance between two consecutive APs didn’t exceed 0.76 seconds (this value was calculated from the histogram of interspike intervals as the right boundary of the histogram’s main peak). The corresponding epoch started 0.5 seconds prior to the first action potential of the burst. Silent epochs were randomly sampled from the between-burst periods. Averaged EEG signal at each time point was calculated as arithmetic mean of all the signals in the class

Table 1

EEG classification results

	Precision, %	Recall, %	Accuracy, %	Area under the ROC curve
Class 0 (“spontaneous”)	73±5	68±2	71±4	0.76±0.05
Class 1 (“silent”)	69±5	74±6		

Average values and standard deviations are given. n = 8 cells

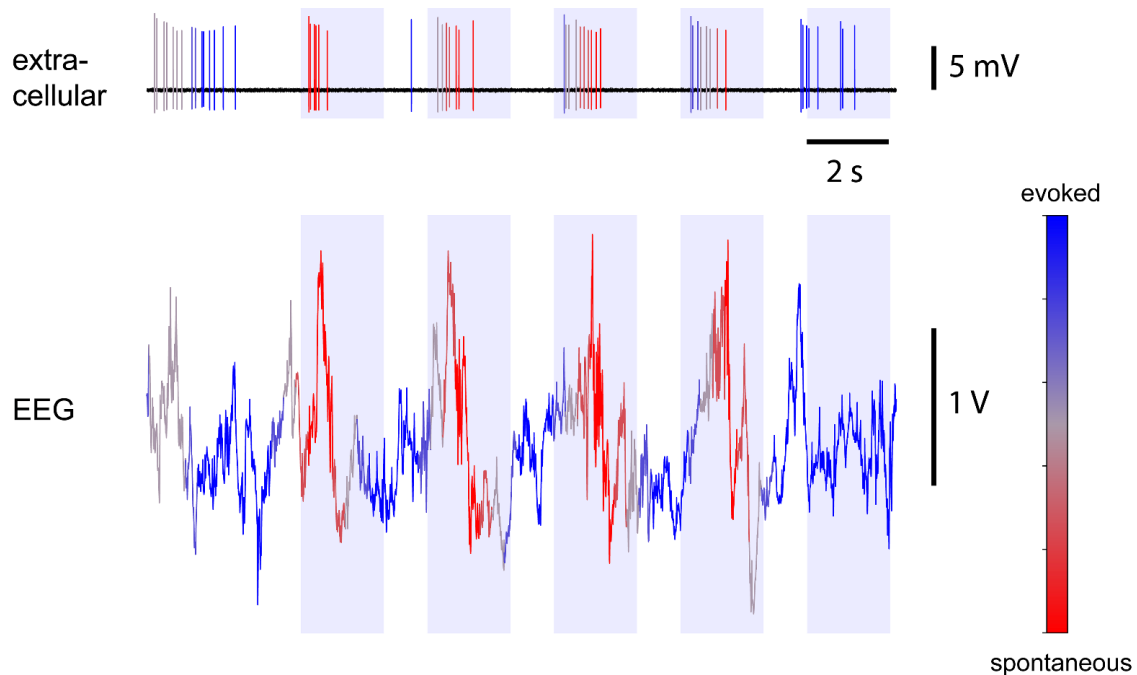
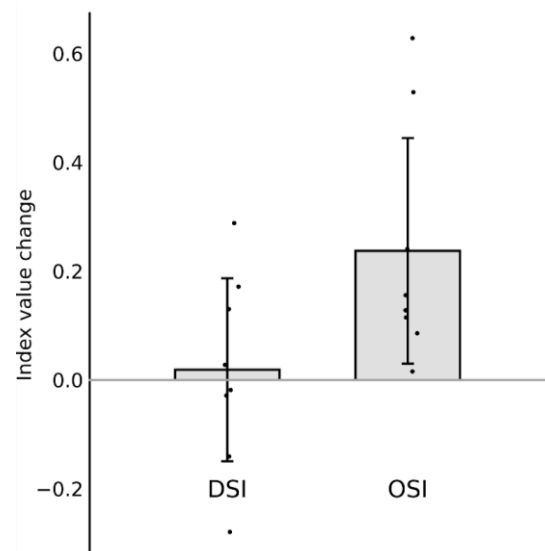


Fig. 3. An example of EEG analysis performed on stimulation data. Top: extracellular recording from a V1 neuron, bottom: simultaneous EEG recording, on which analysis has been performed. Color scale represents the EEG classification results, according to which each data point is assigned to one of the two classes, with probability ranging from 0 (“spontaneous” class, red), to 1 (“silent”, blue). Light blue shading corresponds to 2 second long stimulus (moving grating) presentations

Fig. 4. Selectivity indices’ change after the cleansing procedure had been applied. Bars show the average change of direction selectivity index (DSI) (nonsignificant change) and orientation index (OSI) (significant increase) values after exclusion of spontaneous action potentials. Individual results are indicated by black dots ($n = 8$ cells). Errorbars correspond to one standard deviation



trained on another cell recorded from the same animal. It indicates that the effect of the excitation source is indeed general and uniform across V1 cells, although it might change as anesthesia depth slightly varies with time. Besides, there is no doubt, that each individual

cell’s response to the same stimulus would be unique as it is modulated by local network interactions.

Then, we made an auxiliary algorithm to perform a continuous EEG classification within a sliding window, as described in Methods, on

the data that had been recorded during visual stimulation. An example result of such classification is given in Fig. 3. Here, color scale encodes the certainty of prediction. We can see that our classifier is able to detect EEG patterns similar to those seen alongside spontaneous bursts. Specifically, low-frequency (the peak) and high-frequency (the descending “comb”) components are both necessary for detection.

Orientation selectivity of the cell improves after the cleansing algorithm has been applied to the stimulation data. V1 neurons are known to be tuned to particular orientations of visual stimuli, that is each of them has a preferred stimulus orientation that elicits the greatest firing rate. As a matter of fact, this is why gratings or stripes are commonly used as stimuli. Simple cells of V1 are usually direction selective as well, meaning that their response at the preferred direction movement is higher than at the opposite one. Accordingly, for a particular cell, strength of its selectivity can be characterized by various measures, for example, OSI for orientation and DSI for direction (for the mathematical definitions, see Methods).

To assess the effect of the cleansing procedure, we calculated these two indices before and after it was applied for each cell. We found that OSI increased significantly ($\Delta\text{OSI} = 0.25$, $\sigma = 0.21$, $p = 0.0096$ for one-sided t-test; $p = 0.22$ for Shapiro-Wilk test for normality), while the change of DSI was not significant ($\Delta\text{DSI} = 0.02$, $\sigma = 0.17$, $p = 0.78$ for one-sided t-test; $p = 0.99$ for Shapiro-Wilk test) (see Fig. 4). These results indicate that indeed, for most of the cells the apparent orientation selectivity improves after the spontaneous activity has been excluded by means of the procedure we propose here. As for the direction selectivity, the apparent index values could both be greater or less than true values depending on whether the cell was simple or complex (we did not test that). However, we can trust the resulting change, as the orientation selectivity for these cells improved.

Discussion

General principles of network interactions in the brain remain elusive. In this study, we

presumably uncovered the share of general influences that encompass both primary visual cortex and parietal cortex. Indeed, EEG features from the latter enabled us to predict a great deal of neuronal spontaneous activity that arises in the former. Often the characteristic EEG pattern represented a slow wave crowned with descending high-frequency fluctuations.

Similar EEG synchronization events had been documented by Steriade *et al.*, 1993 (e.g., Fig. 6, Fig. 8a) in various cat neocortex areas. These authors showed that the slow rhythm is generated in the cortex, coexists with thalamic spindles and is modulated (not induced though) by the thalamus. Importantly, they also demonstrated that in cats such slow EEG activity was not due to the effect of the anesthetic, including urethane. However, there is lack of similar data on rodents.

Speaking of interconnections between spontaneous neuronal activities in different cortex areas, it is noteworthy that the said slow rhythms encompass all neocortical neurons (Volgushev *et al.*, 2006). We might expect to see a high degree of synchronization across the major part of the mouse cortex tissue, since it is quite small. In our case, presumably, spontaneous activity and EEG rhythmical activity were both manifestation of the same phenomenon-regular outbreaks of synchronized slow neuronal activity (Ruiz-Mejias *et al.*, 2011). This assumption is supported by the fact that different V1 cells from the same animal are activated along with similar EEG patterns. However, the trained model could not be successfully applied to a different cell in a different animal, but rather our algorithm should be trained for each recorded mouse individually. Most certainly, it is due to the fact that the frequency content of the characteristic associated EEG pattern varied significantly from one animal to another. These observations suggest that, despite having some typical features for the condition, the underlying network activity is still unique for each particular animal. It might be characteristic of the mouse as our experimental subject or of urethane anesthesia on rodents.

Despite the aforementioned variety of the data, the approach that we propose here proved to be efficient enough for all recorded animals, as evidenced by the improvement of neurons' orientation selectivity index. Therefore, removal of spontaneous action potentials from recordings of neuronal activity using our algorithm allows for a more adequate estimation of parameters of neuronal sensory inputs.

Acknowledgements

We thank Ilya Mikheev (HSE University, Russia) for his advice and helpful suggestions on machine learning techniques.

This work was supported by Russian Science Foundation, grant # 20-15-00398.

References

- AL-QEREM A., KHARBAT F., NASHWAN S., ASHRAF S. & BLAOU K. (2020): General model for best feature extraction of EEG using discrete wavelet transform wavelet family and differential evolution. *International Journal of Distributed Sensor Networks*, **16**(3).
- KRONE L.B., YAMAGATA T., BLANCO-DUQUE C., GUILLAUMIN M., KAHN M.C., VAN DER VINNE V., MCKILLOP L.E., TAM S., PEIRSON S.N., AKERMAN C.J., HOERDER-SUABEDISEN A., MOLNÁR Z. & VYAZOVSKIY V.V. (2021): A role for the cortex in sleep-wake regulation. *Nature neuroscience*, **24**(9), 1210–1215.
- LEE G. R., GOMMERS R., WASILEWSKI F., WOHLFAHRT K. & O'LEARY A. (2019): PyWavelets: A Python package for wavelet analysis. *Journal of Open Source Software*, **4**(36), 1237.
- LUCZAK A., BARTHÓ P., MARGUET S.L., BUZSÁKI G. & HARRIS K.D. (2007): Sequential structure of neocortical spontaneous activity in vivo. *Proceedings of the National Academy of Sciences* **104**(1), 347–352.
- MAZUREK M., KAGER M. & VAN HOOSER S. D. (2014): Robust quantification of orientation selectivity and direction selectivity. *Front. Neural Circuits* **8**:92.
- MCVEA D. A., MURPHY T. H. & MOHAJERANI M. H. (2016): Large scale cortical functional networks associated with slow-wave and spindle-burst-related spontaneous activity. *Frontiers in neural circuits*, **10**, 103.
- PEDREGOSA F., VAROQUAUX G., GRAMFORT A., MICHEL V., THIRION B., GRISEL O., BLONDEL M., PRETTENHOFER P., WEISS R., DUBOURG V., VANDERPLAS J., PASSOS A., COURNAPEAU D., BRUCHER M., PERROT M. & DUCHESNAY É. (2011): Scikit-learn: Machine Learning in Python, *JMLR* **12**(85), 2825–2830.
- RUIZ-MEJIAS M., CIRIA-SUAREZ L., MATTIA M. & SANCHEZ-VIVES M. V. (2011): Slow and fast rhythms generated in the cerebral cortex of the anesthetized mouse. *Journal of Neurophysiology*, **106**:6, 2910–2921.
- STERIADE M., NUÑEZ A. & AMZICA F. (1993): Intracellular analysis of relations between the slow (< 1 Hz) neocortical oscillation and other sleep rhythms of the electroencephalogram. *The Journal of Neuroscience*, **13**(8), 3266–3283.
- VOLGUSHEV M., CHAUVETTE S., MUKOVSKI M. & TIMOFEEV I. (2006): Precise long-range synchronization of activity and silence in neocortical neurons during slow-wave oscillations [corrected]. *The Journal of Neuroscience*, **26**(21), 5665–5672.